

# THE 4TH INTERNATIONAL CONFERENCE ON ALUMINUM ALLOYS

## SURFACE OXIDE OF BRAZE CLAD ALUMINIUM

I. Olefjord<sup>1</sup>, T. Stenqvist<sup>2</sup>, and Å. Karlsson<sup>2</sup>

<sup>1</sup>Chalmers University of Technology, S-412 96 Gothenburg, Sweden

<sup>2</sup>Gränges Technology Centre, S-612 81 Finspong, Sweden

### Abstract

The composition and the thickness of the surface oxide products formed during annealing of braze clad aluminium for vacuum brazing were analysed using ESCA, Auger, and SEM. The core and the clad layer were AA 3003 and AA 4004, respectively. The surfaces of cold rolled, plant annealed (365°C), and laboratory annealed (300-500°C) material were studied. Both mill finish and polished surfaces were analysed.

The cation content of Mg<sup>2+</sup> in the oxides formed during cold rolling and during plant annealing is 8 and 28 at.%, respectively. The Si<sup>4+</sup> content of the oxides is a few per cent. On polished samples Mg is enriched in the inner part of the oxide. In the temperature range 400 to 500°C the Mg<sup>2+</sup> content increases from 40 to 90 at. %.

The thickness of the oxides formed during cold rolling and mill annealing is 33 and 46 Å, respectively. Laboratory annealing of polished material at 300 and 400°C gives 43 and 56 Å thick oxides, respectively. The oxide formed above 450°C is non-uniform in thickness; islands of Mg-oxide are formed. After annealing at 500°C Mg oxide particles occur along phase boundaries and also form a mosaic pattern, reminiscent of a subgrain structure. Auger analysis shows that the average thickness of the oxide formed at 500°C is in the range 250 to 500 Å. However, the metallic state of Al is detected by ESCA showing that parts of the surface are covered with a very thin Al<sub>2</sub>O<sub>3</sub> layer.

### Introduction

Vacuum brazing is a common method of joining aluminium especially for heat exchangers. Usually the filler metal is supplied via a thin clad layer on an aluminium alloy core. The braze filler alloy is often AA 4004 containing 10 wt.% Si and 1.5 wt.% Mg. Its solidus temperature is 555°C and its liquidus temperature is about 590°C dependent on the exact composition of the alloy. The Mg in the filler promotes brazing by modifying the surface oxide and causing oxide film disruption. Molten filler metal penetrates through the oxide cracks as exudations and eventually macroscopic filler flow occurs. After disruption of the oxide film Mg, due to its higher vapour pressure, evaporates and improves the vacuum in the brazing furnace.

The mechanism of vacuum brazing has been extensively studied, e.g. [1, 2]. The effect of different pretreatments, including preoxidation, on the oxide disruption and formation of exudations has been studied in [3]. Preoxidation of Mg impairs its function during brazing. The aim of the present work is to study the oxidation behaviour of the clad material at temperatures and times which are relevant for production of the brazing material.

### Experimental

The test material was produced by Finspong Aluminium. The total thickness was 1 mm and the cladding thickness was 0.1 mm. Both plant annealed and laboratory annealed material was studied. The composition of core and cladding is shown in Table I. The surface finishes and annealing temperatures are shown in Table II. The samples were heated in air at 50°C/h to the annealing temperature. Time at temperature was 1 h.

Table I Composition, wt. %, of the core and the cladding alloys.

		Si	Fe	Cu	Mn	Mg
<u>Plant annealed</u>						
Core	AA3003	0.12	0.47	0.12	1.09	<0.01
Clad layer	AA4004	10.0	0.21	0.01	0.07	1.34
<u>Laboratory annealed</u>						
Core	AA3003	0.16	0.50	0.12	1.10	<0.01
Clad layer	AA4004	9.5	0.34	0.02	0.03	1.32

The samples, 10 x 10 mm<sup>2</sup>, were analysed by ESCA (PHI 5500), Auger (PHI 660), and SEM (Jeol 840). The ESCA and Auger analyses were performed in order to obtain the chemical composition and the thickness of the oxide layers. The in depth composition was determined using angle-dependent ESCA analysis and ion etching.

Table II The surface finishes and annealing temperatures

Surface finish	Annealing temperature(°C)					
	RT	300	365	400	450	500
Mill finish	+	+	+	+	+	+
Polished	+	+		+	+	+

\* Plant annealed; all others laboratory annealed

### Results

Figure 1 shows SEM micrographs of the surfaces. The mill finish surfaces show normal rolling lines. The polished surfaces reveal Si and Mg<sub>2</sub>Si particles, which were mostly covered by aluminium during rolling. MgO particles (the identification is discussed later) are visible after annealing at 450 and 500°C on both the mill finish and polished samples. The MgO particles occur preferentially at surface defects and at phase boundaries, Figs. 1 d-f, i-k. They also form a mosaic pattern on polished samples, Figs. 1 j, k.

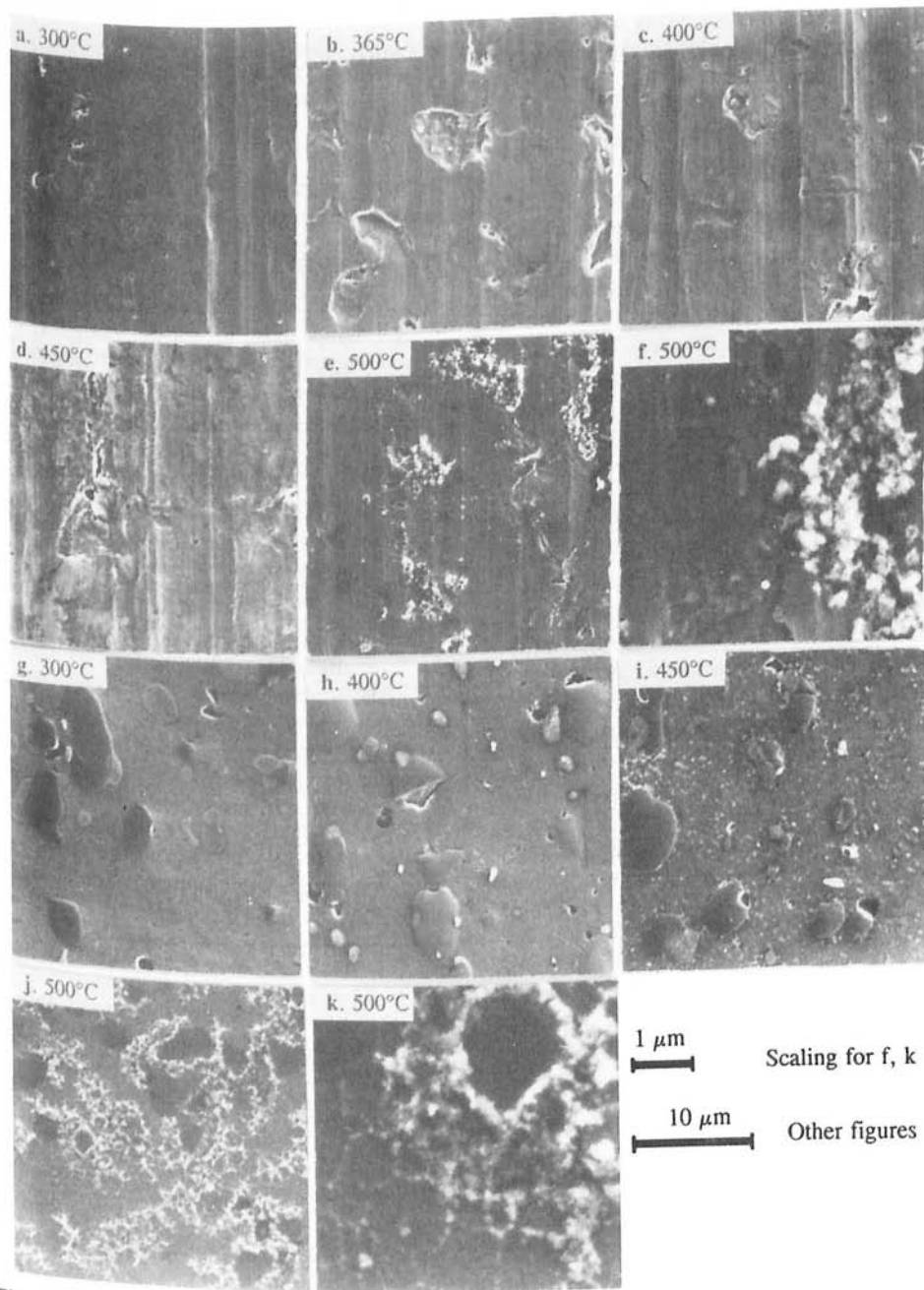


Figure 1. SEM micrographs of surfaces. a. - f. mill finish, g. - k. polished surfaces. Annealing: b. plant annealed, all others lab annealed.

In Fig. 2 ESCA survey scans are shown for three samples: a) polished and exposed to ambient atmosphere at RT; b) plant annealed at 365°C; c) mill finish and annealed at 500°C. The spectra show signals from Al, Mg, Si, O, C, and Cu. Even low intensity signals from N, Cl, Na and Ca occur; these elements are contaminants and will not be further discussed. Mainly Al and Si oxides are formed on the polished and room temperature exposed sample. The plant annealed sample shows strong signals from Mg and Al oxides. Annealing the mill finish sample at 500°C causes formation of mainly MgO.

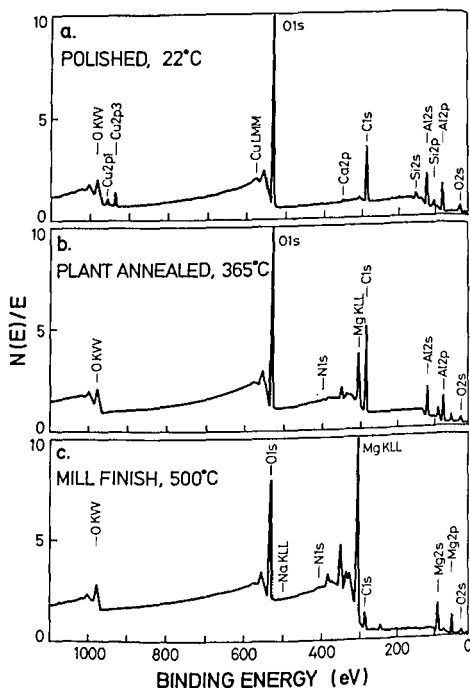
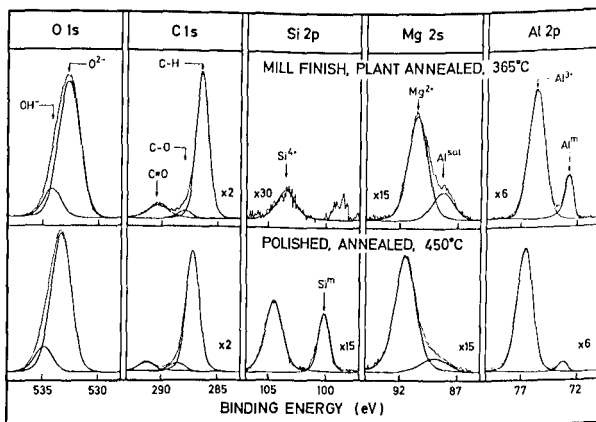


Figure 2. ESCA survey scans:  
 a) polished sample exposed to atmosphere at RT  
 b) plant annealed at 365°C  
 c) lab. annealed at 500°C

Examples of high resolution ESCA spectra are shown in Fig. 3: a) mill finish and plant annealed at 365°C; b) polished and annealed at 450°C. The spectra show both the metallic, and the oxide states of Al and Si. Mg can only be detected in its divalent state. The intensity of the Si signal recorded from the polished sample is markedly higher than the signal from the mill finish because the Si particles are uncovered by polishing. The fact that the metallic states of Al and Si can be detected shows that the oxide is at least partly thin. The oxide thickness can be calculated from the intensity ratio between the oxide and the metallic states. The oxygen signals show two peaks indicating that hydroxide is present on the surface. The contribution of the OH<sup>-</sup> signal to the total

Figure 3.  
 ESCA spectra recorded from:  
 a) mill finish, plant annealed at 365°C  
 b) polished, lab. annealed at 450°C



oxygen signal is relatively low compared to the contribution from  $O^{2-}$ . The carbon signals represent carbonaceous compounds present as contaminants on the surface.

Figure 4 shows oxygen ion etching profiles recorded by Auger spectroscopy of mill finish material (and one polished). The oxide thickness is estimated from the etch depth at which the intensity of the oxygen signal has decreased to half of its maximum value. The etching rate of the ion gun was calibrated on  $Ta_2O_5$  and converted to the etching rate of  $Al_2O_3$  [4]. The figure shows that the oxide products formed at temperatures up to 300°C are about 35 Å. The oxides formed during plant annealing at 365°C and during lab annealing at 400°C are 50 and 75 Å, respectively. Annealing of the mill finish material at 450°C gives a 95 Å thick oxide. At 500°C the oxygen profile is relatively flat showing that the thickness of the oxide products varies over the surface. The oxygen profile gives in fact the thickness distribution of the surface oxide. The maximum thickness of the oxide (MgO) formed at 500°C is about 500 Å (not shown in the figure).

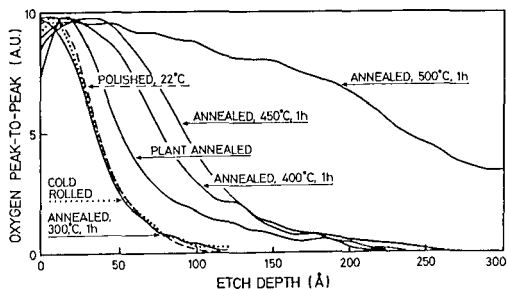


Figure 4. Auger profiles after different annealings.

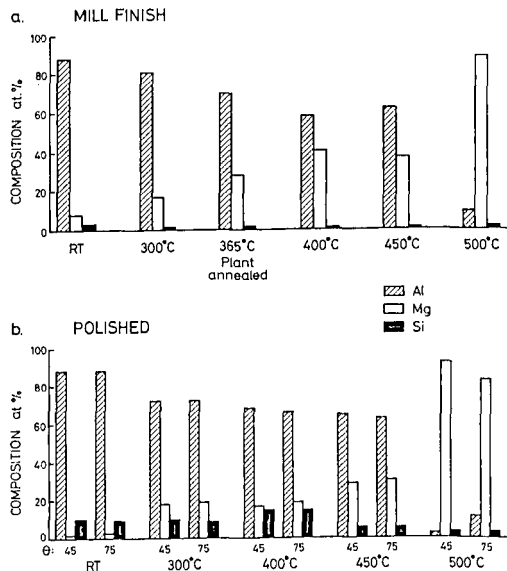


Figure 5. The composition of oxides formed in the temperature range room temperature to 500°C: a) mill finish; b) polished samples ( $\theta$  is the take off angle).

The composition and the thickness of the oxide can be determined from the measured ESCA intensities. The photoelectron yield constants, the attenuation lengths of the photoelectrons and the densities of the metals and the oxides have to be known. Details are given in [5].

Figure 5 shows the cation content of the oxides formed on the mill finish and on the polished samples determined from the ESCA results.  $Al^{3+}$  is the dominating cation in the oxide formed on both surface conditions at temperature up to 400°C. The  $Mg^{2+}$  content increases monotonously with the annealing temperature. The measured  $Mg^{2+}$  content (cation concentration) of the polished sample exposed to atmosphere at RT is 3 at.%. The  $Mg^{2+}$  content of the oxide formed on the cold rolled surface is 8 at.%. The oxide formed during plant annealing, 365°C, contains 28 at.%  $Mg^{2+}$ . Annealing of the mill finish material at 300

and 400°C gives 17 and 41 at.% Mg<sup>2+</sup>, respectively. At 450 and 500°C the Mg<sup>2+</sup> contents are 62 and 89 at.%, respectively. The oxide formed on the polished material at 400 and 450°C contains noticeably less Mg<sup>2+</sup> than the oxide on the mill finish material. At 500°C Mg<sup>2+</sup> is the dominating cation in the oxide; the Mg<sup>2+</sup> content is about 90 at.%. Analysis after a slight ion etching of all samples annealed up to 400°C indicates that Mg<sup>2+</sup> is enriched at the oxide/metal interface. However, angle dependent ESCA measurements do not show this Mg distribution. Auger mapping indicates that the Si particles are covered only with SiO<sub>2</sub>. The difference in Si<sup>4+</sup> concentrations between the two surface conditions shows that the Si<sup>4+</sup> content in the oxide formed on the matrix is low.

The oxide thicknesses obtained by both ESCA and Auger are shown in Fig. 6.

It was assumed that a mixed (Al, Mg) oxide covers the matrix and that SiO<sub>2</sub> covers the Si particles. The oxide thickness on the matrix increases with annealing temperature. At room temperature (cold rolled and polished) the oxide thickness measured by ESCA and Auger is 33 ± 4 Å. At 300 and 400°C the oxides on the polished samples have increased to 43 and 56 Å, respectively. The oxide thickness of the plant annealed sample is 46 Å. The thickness of the oxide formed at 450°C was found by Auger to be 95 Å. The measured thicknesses (half maximum intensity) of the oxides formed on the mill finished and polished samples at 500°C are 240 and 500 Å, respectively.

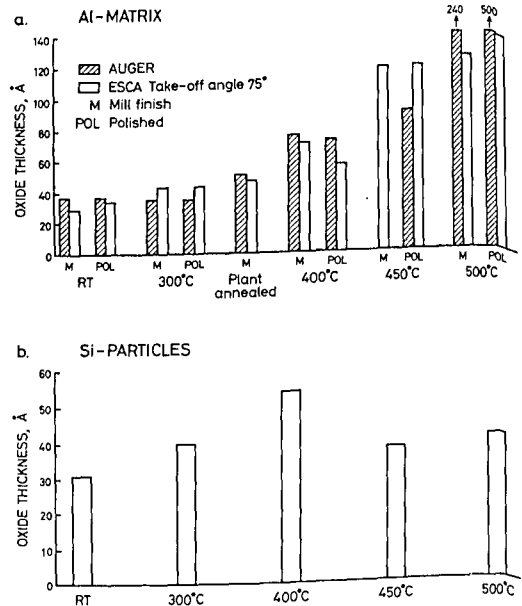


Figure 6. The thickness of oxides formed on: a) the matrix of the alloy; b) the Si particles.

### Discussion

Oxidation during processing and handling has to be controlled in order to guarantee proper brazing behaviour. Oxidation of this type of alloy for 4 h at 475°C had a severe effect on the melting behaviour [3]. The present study shows that the thickness and the Mg<sup>2+</sup> content of the oxide increases markedly in the temperature range 450 to 500°C. The Mg<sup>2+</sup> content of the oxide on mill finish material at 500°C is 90 at.%. The oxide thickness formed at 450°C is about 100 Å and it is in the range 250 to 500 Å after annealing at the higher temperature. The SEM micrographs show MgO particles on the surface after oxidation at 450°C and the coverage of these particles increases with the temperature. It has been shown that these particles consist of MgO [6, 7]. Small amounts of spinel, MgAl<sub>2</sub>O<sub>4</sub>, may also be formed [7]. The mosaic pattern of MgO particles is reminiscent of a subgrain structure, Figs. 1 j-k.

Cracks in the oxide can be induced by the difference in thermal expansion between the oxide and the matrix allowing Mg to reach the surface.

The morphology of the oxide at temperatures above 400°C is illustrated schematically in Fig. 7. The thin oxide is a continuous film of  $\gamma\text{-Al}_2\text{O}_3$  [8]. MgO particles are nucleated at the metal oxide interface [2] and grow outwards. These particles are too small to be seen in the SEM photos. The ion sputtering experiments show higher  $\text{Mg}^{2+}$  concentration after a slight etching. The fact that the angle dependent measurements do not clearly show any angle dependence of the  $\text{Mg}^{2+}$  content indicates that  $\text{Mg}^{2+}$  occurs as discrete particles. At increased temperatures the particles grow in size and number.

The formation of MgO at 400 and 450°C is dependent on the surface condition; at both temperatures the measured  $\text{Mg}^{2+}$  contents on the polished surfaces were found to be about half of the  $\text{Mg}^{2+}$ -contents of the mill finish samples. It is suggested that nucleation and growth of MgO is limited on the polished surface due to formation of a more protecting  $\text{Al}_2\text{O}_3$  layer. The mill finish surface has a high defect density and is partly covered with non-protecting hydroxide compounds. However, at 500°C the oxide formed on the polished sample becomes thicker than the oxide on the mill finish. This is probably due to the fact that the enrichment of  $\text{Mg}^{2+}$  is limited at lower temperatures during the heating and thereby the driving force for oxidation of Mg becomes high at 500°C. This reaction pattern is consistent with the result from thermogravimetric analysis [9] of this test material showing that the degassing temperature of Mg is dependent on the pretreatment of the material; on a polished sample the Mg degassing starts at 496°C while it is delayed to 531°C on the plant annealed sample.

The oxide formed on aluminium at temperatures lower than 400°C is amorphous [8]. Quantitative surface analyses [10, 11] of the oxide layers formed on pure aluminium during oxidation for 5 h at room temperature and at 250°C have shown that the thicknesses of the oxides are 15 and 22 Å, respectively. In this work we found using the same analytical procedure that the thickness of the oxide formed at room temperature is about 30 Å. The increased oxide thickness can not be due only to the longer exposure time. Instead, the increased oxide thickness is probably due to handling of the material in air, which causes hydration of the oxide and growth of the oxide products [5, 11]. A hydroxide layer is less protective than a pure oxide against further oxidation. The thin hydroxide layer is not easily analysed by the ESCA-technique because the hydroxide is decomposed in vacuum [5], therefore the low intensity of the  $\text{OH}^-$  signals in Fig. 3. The growth of the oxide may also be due to doping of  $\text{Al}_2\text{O}_3$  with  $\text{Mg}^{2+}$  ions. The increased defect concentration increases the diffusion rate of the ions and thereby the oxide growth. Surface analysis [12] of aluminium foil containing 48 ppm Mg has shown that  $\text{Mg}^{2+}$  ions are enriched in the oxide.

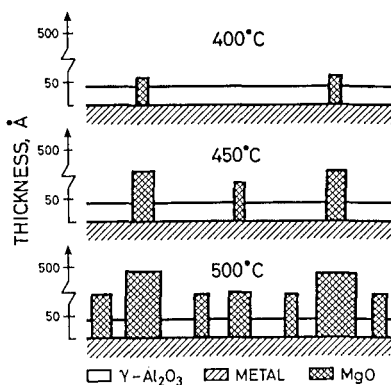


Figure 7. Morphology of the oxide at annealing above 400°C; schematically.

## Conclusions

The thickness of the oxide formed on AA4004 in connection with cold rolling and plant annealing is 33 Å and 46 Å, respectively. The oxide formed during heat treatment in air at 500°C is 250 to 500 Å thick.

The Mg<sup>2+</sup> content (cation concentration) of the surface oxide formed during cold rolling, plant annealing, and heat treatment at 500°C is 8, 28, and 90 at. %, respectively.

MgO particles appear in SEM micrographs after annealing at 450°C and higher temperatures. They are nucleated at phase boundaries and defects.

The thickness of the oxide formed during annealing at 500°C is non-uniform. Between thick (~ 500 Å) particles of MgO a thin film (~ 50 Å) of Al<sub>2</sub>O<sub>3</sub> exists.

## Acknowledgements

This work was performed for Finspong Aluminium AB. We thank Kent Schölin, Lars Östensson, Göran Lundblad, and Yvonne Olefjord for their valuable contributions.

## References

1. W. L. Winterbottom and G. A. Gilmour, J. Vacuum Sci. Techn. **13**, (1976), 634.
2. D. K. Creber, J. Ball and D. J. Field, "A Mechanistic Study of Aluminum Vacuum Brazing," SAE Technical Paper Series, 870185, 1987.
3. B. McGurran, M. G. Nicholas and Å. Karlsson, Aluminium Technology '86, ed. T. Sheppard (London: The Institute of Metals, 1986), 528.
4. I. Olefjord, H. J. Mathieu and P. Marcus, Surf. and Interf. Analysis **15**, (1990), 681.
5. A. Nylund and I. Olefjord, Surf. and Interf. Analysis **21**, (1994), 283.
6. K. Wefers, Aluminium **57**, (1981), 722.
7. M. H. Zayan, O. M Jamjoom and N. A. Razik, Oxidation of Metals **34**, (1990), 323.
8. G. D. Preston and L. L. Bircumshaw, Phil. Mag. **22**, (1936), 654.
9. R. Kiusalaas, "Thermogravimetric analysis of magnesium evaporation". (Report IM-3016, Swedish Institute for Metals Research, 1993.)
10. P. Marcus, C. Hinnen and I. Olefjord, Surf. and Interf. Analysis **20**, (1993), 923.
11. I. Olefjord and A. Nylund, Surf. and Interf. Analysis **21**, (1994), 290.
12. I. Olefjord and Å. Karlsson, Aluminium Technology '86, ed. T. Sheppard (London: The Institute of Metals, 1986), 383.